Supplementary Information

## Intermetallic wetting enabled high resolution liquid metal patterning for 3D and flexible electronics

Lucy Johnston[a], Jiong Yang[b], Jialuo Han[b], Kourosh Kalantar-Zadeh[b]*, Jianbo Tang[b]*

[a]James Watt School of Engineering, University of Glasgow, Glasgow, G12 8QQ, Scotland

[b]School of Chemical Engineering, University of New South Wales (UNSW), Sydney, NSW, 2052 Australia

*Corresponding authors. Email: k.kalantar-zadeh@unsw.edu.au and jianbo.tang@unsw.edu.au
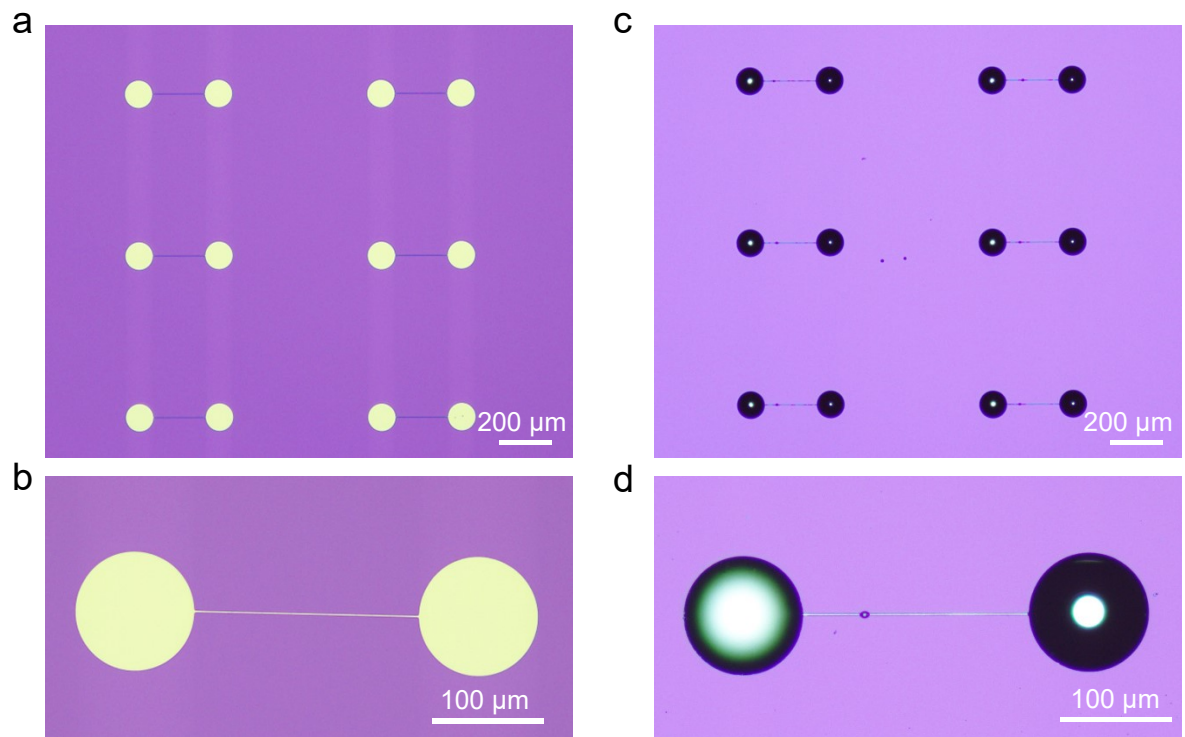
**Fig. S1.** (a, b) Au precursory patterns with 1.3 µm line width. Two circular pads at the line ends were designed for the conductivity measurement. (c,d) Liquid metal patterns after touch transfer using samples in a and b.
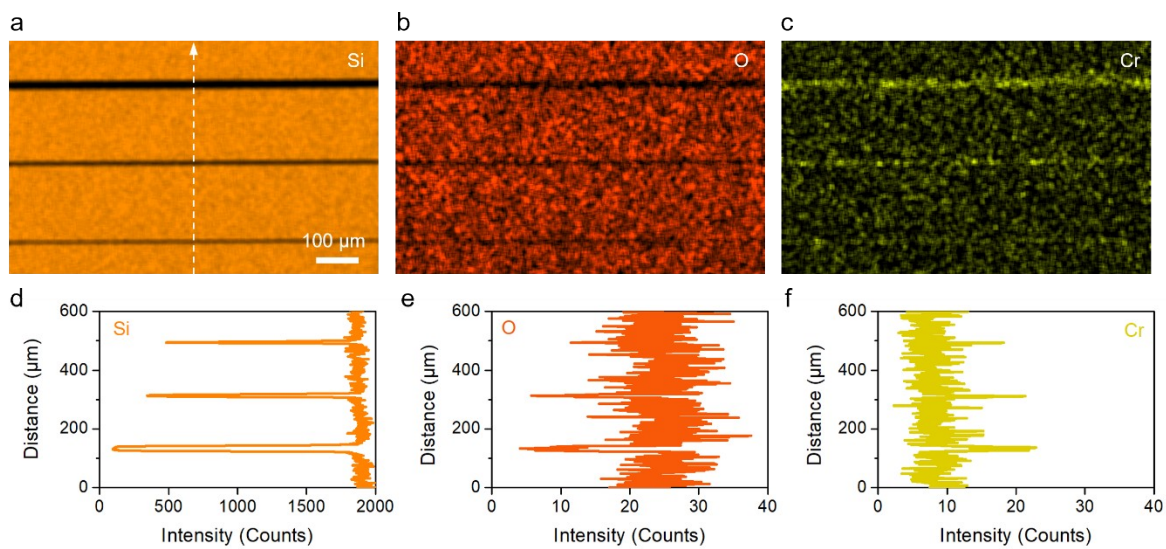
**Fig. S2.** EDX mapping of Si (a), O (b), and Cr (c) as indicated. Scalebars: 100 µm. (d-f) The EDX line mapping intensity of Si, O, and Cr, respectively, along the dashed arrow in a.
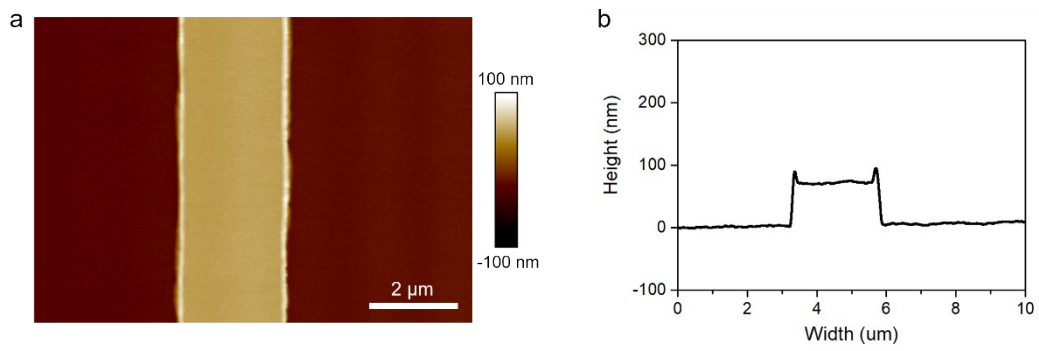
Fig. S3. (a) AFM image showing the thickness of the deposited Au layer and (b) its cross sectional profile. During thin film deposition, a 5 nm Cr layer was first deposited for adhesion enhancement followed by depositing a 50 nm Au layer.
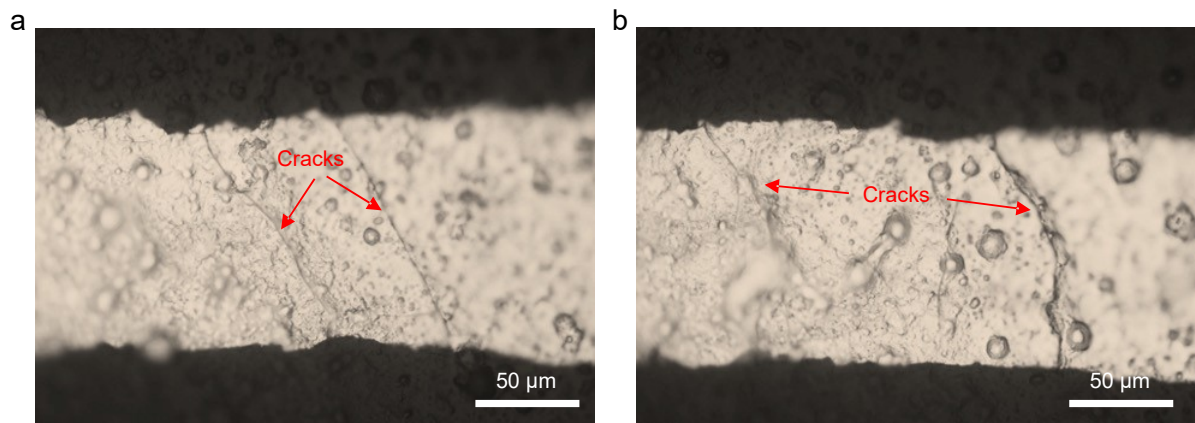
Fig. S4. (a, b) Au tracks on PDMS substrate with frequently observed cracks along the entire width, due to the flexible nature of the substrate onto which they were deposited. These cracks effectively disconnect the Au tracks which become non-conductive.
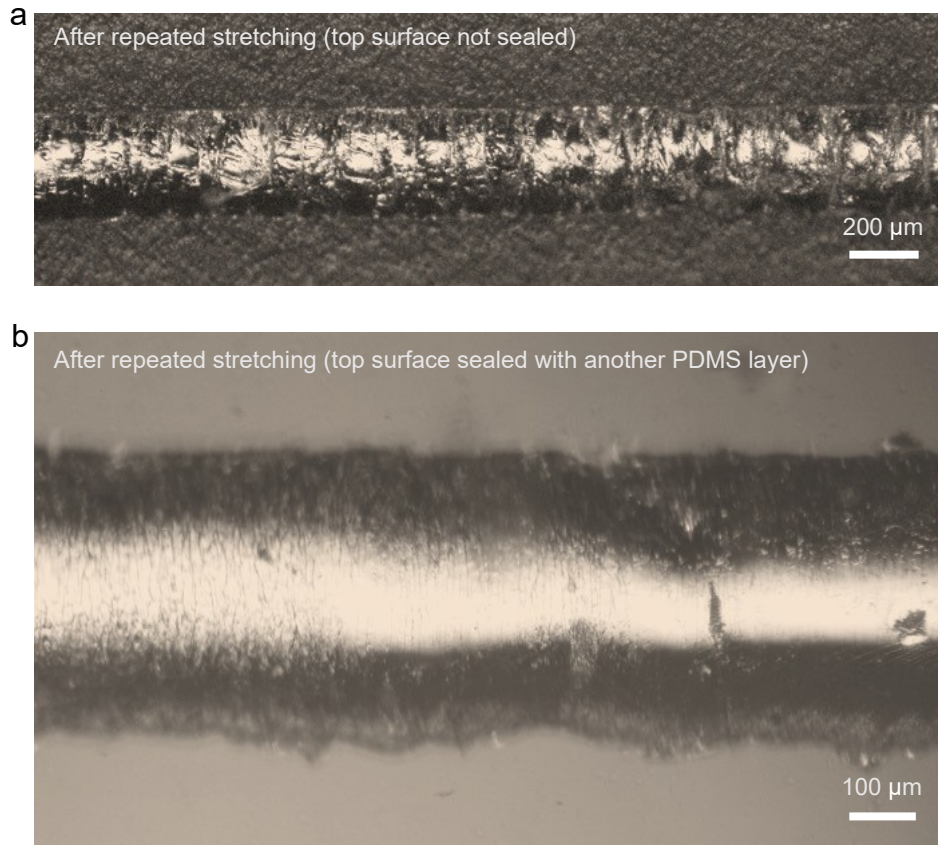
Fig. S5. (a) A EGaIn track, with top surface non sealed, displaying intensive large wrinkles on its surface after repeated stretching. (a) A EGaIn track, with top surface sealed with another PDMS layer, showing insignificant surface appearance change and small surface wrinkles (in comparison to the non-sealed sample) after repeated stretching.
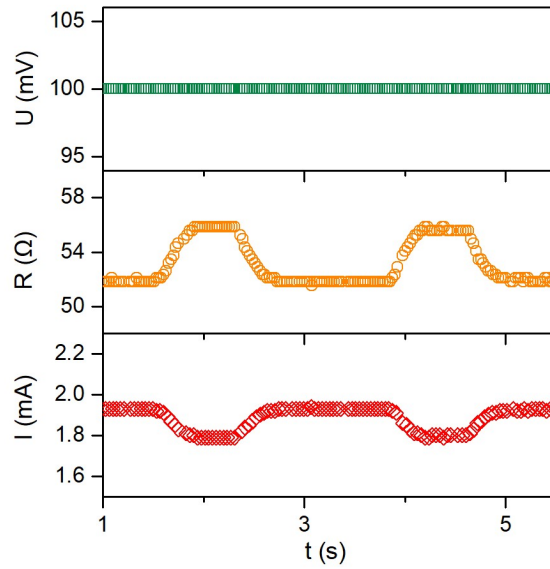
Fig. S6. The measured time-dependent resistance and current changes under constant voltage (100 mV) bias during two cycles with a smaller finger bending angle (60 degree) that Fig. 6e. The current and resistance changes are about 8% of the original values, which are smaller than the changes at the 90-degree bending angle in Fig. 6e.

Table S1. Comparative table comparing conventionally used liquid metal patterning techniques. The type of liquid metal used is listed, as well as the highest resolution achieved with the named method, substrates used and their ability to be applied to flexible and 3D substrates.

Method	Liquid Metal	Resolution	Substrate Materials	Flexible substrate	Non-planar substrate	Year	Ref
Current Work	EGaIn	2 μm	SiO_2, glass, plastic, stainless steel, PDMS	Y	Y	2021	
Direct Writing	GaIn	2 mm	Glass, silica gel plate, plastics, paper, glass fibre cloth.	Y	N	2012	1
	GaIn	1.5 mm	Coated paper	Y	N	2013	2
	GaIn	100 μm	PVC	Y	N	2014	3
	EGaIn	1.9 μm	Si, glass, PDMS, PET	Y	N/A*	2019	4
Spray Printing	Galinstan	30 μm	PDMS, PET, glass	Y	Y	2020	5
	EGaIn	20 μm	PDMS	Y	N	2017	6
	GaIn	50 μm	PDMS, PVC	Y	N	2015	7
	EGaIn	1 mm	Ecoflex	Y	N	2018	8
	EGaIn	300 μm	PMA glue, paper	Y	N	2018	9
Injecting	Galinstan	70 μm	Silicon wafer, PDMS	Y	N	2017	10
	EGaIn	118 μm	PDMS	Y	N	2019	11
Imprinting	EGaIn	0.18 μm	PDMS	Y	N	2020	12
	EGaIn	2 μm	PDMS	Y	N	2014	13
Selective Wetting	Galinstan	2 μm	PDMS	Y	N	2017	14
	EGaIn	40 μm	PDMS	Y	N	2018	15
Electrowetting	EGaIn	~ 60 μm	SiO_2, Parylene C on glass	N	N/A*	2019	16
Droplet Microprinting	EGaIn	340 μm	Silicone elastomer	Y	N	2013	17
Vacuum Filling	EGaIn	5 μm	PDMS	Y	N	2017	18
	Galinstan	250 μm	PVA	Y	N	2019	19
Laser assisted prototyping	GaIn	>150 μm	PDMS	Y	N	2014	20

*Method allows for the fabrication of free-standing liquid metal structures.

References

1. Y. Gao, H. Li and J. Liu, *PLOS ONE*, 2012, **7**, e45485.
2. Y. Zheng, Z. He, Y. Gao and J. Liu, *Sci. Rep.*, 2013, **3**, 1786.
3. Y. Zheng, Z.-Z. He, J. Yang and J. Liu, *Sci. Rep.*, 2014, **4**, 4588.
4. Y.-G. Park, H. S. An, J.-Y. Kim and J.-U. Park, *Sci. Adv.*, 2019, **5**, eaaw2844.
5. T. H. Park, J.-H. Kim and S. Seo, *Adv. Funct. Mater.*, 2020, **30**, 2003694.
6. T. Kim, K. Kim, S. Kim, J. Lee and W. Kim, *J. Microelectromech. Syst.*, 2017, **26**, 1244-1247.
7. Q. Wang, Y. Yu, J. Yang and J. Liu, *Adv. Mater.*, 2015, **27**, 7109-7116.
8. R. Guo, X. Wang, W. Yu, J. Tang and J. Liu, *Sci. China Technol. Sci.*, 2018, **61**, 1031-1037.
9. R. Guo, J. Tang, S. Dong, J. Lin, H. Wang, J. Liu and W. Rao, *Adv. Mater. Technol.* , 2018, **3**, 1800265.
10. Y. Gao, H. Ota, E. W. Schaler, K. Chen, A. Zhao, W. Gao, H. M. Fahad, Y. Leng, A. Zheng, F. Xiong, C. Zhang, L.-C. Tai, P. Zhao, R. S. Fearing and A. Javey, *Adv. Mater.*, 2017, **29**, 1701985.
11. R. Wang, L. Gui, L. Zhang, Z. He, M. Gao, S. Chen, X. Zhou, Y. Cui and Z. Deng, *Adv. Mater. Technol.*, 2019, **4**, 1900256.
12. M.-g. Kim, D. K. Brown and O. Brand, *Nat. Commun.*, 2020, **11**, 1002.
13. B. A. Gozen, A. Tabatabai, O. B. Ozdoganlar and C. Majidi, *Adv. Mater.*, 2014, **26**, 5211-5216.
14. G. Li and D.-W. Lee, *Lab on a Chip*, 2017, **17**, 3415-3421.
15. K. B. Ozutemiz, J. Wissman, O. B. Ozdoganlar and C. Majidi, *Adv. Mater. Interfaces*, 2018, **5**, 1701596.
16. A. M. Watson, A. B. Cook and C. E. Tabor, *Adv. Eng. Mater.*, 2019, **21**, 1900397.
17. A. Tabatabai, A. Fassler, C. Usiak and C. Majidi, *Langmuir*, 2013, **29**, 6194-6200.
18. Y. Lin, O. Gordon, M. R. Khan, N. Vasquez, J. Genzer and M. D. Dickey, *Lab Chip*, 2017, **17**, 3043-3050.
19. L. Teng, S. Ye, S. Handschuh-Wang, X. Zhou, T. Gan and X. Zhou, *Adv. Funct. Mater.*, 2019, **29**, 1808739.
20. T. Lu, L. Finkenauer, J. Wissman and C. Majidi, *Adv. Funct. Mater.*, 2014, **24**, 3351-3356.